

Biochemical Synthesis of Nickel & Cobalt Oxide Nano-particles by using Biomass Waste

Mohib Ullah¹, Asima Naz², Tariq Mahmood³, Muhammad Siddiq⁴, Asghari Bano⁵

^{1,2,4}Department of Chemistry, Quaid-I-Azam University, Islamabad, Pakistan

³Nano Science & Catalysis Division, National Centre for Physics, Quaid-I-Azam University Campus, Islamabad, Pakistan.

⁵Department of Plant Sciences, Quaid-i-Azam University, Faculty of Biological Sciences, Quaid-I-Azam University Islamabad, Pakistan

Abstract: Here in, we are reporting a novel biochemical approach for the formation of nickel and cobalt oxide (NiO and CoO) nanoparticles by using pomegranate peel and fungus at room temperature. We used nickel nitrate hexahydrate $[\text{Ni}(\text{NO}_3)_2 \cdot 6\text{H}_2\text{O}]$ and cobalt nitrate hexahydrate $[\text{Co}(\text{NO}_3)_2 \cdot 6\text{H}_2\text{O}]$ as precursors. Exposure of the biomass waste to aqueous solution resulted in the reduction of the metal ions and formation of nanoparticles (NPs). All nanoparticles were in nano size and were ~40 and ~46 nm respectively. The X-Ray diffraction (XRD) pattern reveals the formation of nickel oxide and cobalt oxide (NiO & CoO) nanoparticles, which shows crystallinity. Brunauer-Emmett-Teller (BET) Surface Area Analysis and Barrett-Joyner-Halenda (BJH) shows pore size and pore volume. Scanning Electron Microscopy (SEM) images reveal that the particles are of spherical and granular shape. Elemental analysis carried out by Energy Dispersion X-rays Spectroscopy (EDX). This is simple and cost-effective biochemical approach for the synthesis of NiO and CoO NPs. These NPs may have a promising role in conversion of organic matter into biofuel and biogas.

Keywords: nickel oxide, cobalt oxide, nanoparticles, fungus, pomegranate peel, biomass.

1 Introduction

Nanomaterials have wide-ranging applications and implications in a variety of areas, including physics, chemistry, electronics, optics, materials science, and the biomedical sciences. Besides, the novel properties exhibited by the metal nanoparticles due to quantum size effects, their synthesis protocol pose a major environmental problem. New applications of nanoparticles and nanomaterials are emerging rapidly (Murphy 2008). The nanomaterials exhibit unique and considerably changed physical, chemical and biological properties when compared to their macro scaled i.e. bulk counterparts (Simone 2002). Nel et al. reported the nanoparticles interaction with biological materials and established a series of nanoparticle/biological interfaces that depend on colloidal forces as well as dynamic biophysicochemical interactions. These interactions lead to the formation of new nanomaterial with control size, shape, surface chemistry, roughness and surface coatings (Nel et al. 2009). Furthermore, evidences suggested that the inorganic nanoparticles are very immense material because of their high surface area, it is easy to enter in cells via pores of plasma membrane proteins at nanoscale size. Apart from this, they have potential properties for sensing and detection of various biological analytes. For instance, the presence of semiconductor metal zinc oxide nanoparticles (< 30 nm) in the biological system have ability to altered biological properties. Zinc oxide nanoparticles have potential applications in various areas including optical, piezoelectric, magnetic and gas sensing and also they exhibit high catalytic efficiency, strong adsorption ability, high isoelectric point (9.5), biocompatibility, and fast electron transfer kinetics for biosensing purposes (Jamieson et al. 2007). The timeliness of "being green and nano" for nanomaterials synthesis is evident from two major reviews that have appeared in 2007 (Mai et al. 2007). It has been recognized for some time that the environmental impact of nanomaterials must be assessed (Colvin 2003).

Most of the synthetic physicochemical methods reported till date are heavily on the use of organic solvents and toxic reducing agents like thiophenol, mercapto acetate, sodium borohydride etc. Most of these chemicals are highly reactive and pose potential environmental and biological risks. With the increasing interest in minimization or elimination of such kinds of hazardous chemicals, the development of biological, biomimetic and biochemical approaches is desirable. Therefore, biological approach has advantages over physicochemical methods because of its clean, non-toxic chemicals, environmentally benign solvents, and user-friendly nature (Albrecht et al. 2006). The use of environmentally benign materials like fungi or the synthesis of silver nanoparticles offers numerous benefits of eco-friendliness and compatibility for pharmaceutical and other biomedical applications as they do not use toxic chemicals for the synthesis protocol (Bhainsa

et al. 2006). Chemical synthesis methods lead to presence of some toxic chemical absorbed on the surface that may have adverse effect in the medical applications. Here we report a novel method for the synthesis and characterization of nickel and cobalt oxide nanoparticles synthesized by pomegranate peel (*Punicagranatum L.*) and *Rhizopusnigricans* fungus. DRS, XRD, BET, EDX and SEM analysis revealed that the nickel and cobalt oxide nanoparticles are monodisperse and with different morphologies as spherical to triangles ranging from ~40 and ~46 nm respectively in size.

2 Experimental

2.1 Methods and Materials

The cobalt nitrate hexahydrate and nickel nitrate hexahydrate [$\text{Co}(\text{NO}_3)_2 \cdot 6\text{H}_2\text{O}$] and [$\text{Ni}(\text{NO}_3)_2 \cdot 6\text{H}_2\text{O}$] were purchased from Sigma Aldrich and Sodium Hydroxide was purchased from Fluka. Pomegranate peel was obtained from local market. *Rhizopusnigricans* Fungus was obtained from bread. All solvents were of analytical reagent grade and were used without further purification. For synthesis of cobalt oxide nanoparticles 1M solution of Cobalt nitrate hexahydrate [$\text{Co}(\text{NO}_3)_2 \cdot 6\text{H}_2\text{O}$] was prepared in 200ml distilled water. A fine piece of pomegranate was added to the 1M solution of cobalt nitrate and this solution along with pomegranate was stirred for 3 hours. After addition of pomegranate 1M solution of NaOH was added as a precipitating agent. The solution was kept overnight and then filtered with whatmann paper. The filtrate was kept in an oven for night and then placed this oven dried filtrate in a furnace at 500°C for 5hrs. Then the calcined sample was ground into fine particles. Similarly For synthesis of nickel oxide nanoparticles 0.5M solution of nickel nitrate hexahydrate [$\text{Ni}(\text{NO}_3)_2 \cdot 6\text{H}_2\text{O}$] in 100ml distilled water. Fine pieces of fungus 5g was added to the 1M solution of Nickel nitrate followed by addition of 1M solution of NaOH and this solution along with fungus was stirred for 5 hours. The solution was kept overnight and then filtered with whatmann paper. The filtrate was kept in an oven for night and then placed this oven dried filtrate in a furnace at 500°C for 5hrs. Then the calcined sample was ground into tiny particles.

2.2 X-ray diffraction measurements

X-Ray diffraction (XRD) measurements of the bio-reduced nickel and cobalt nitrate solutions drop-coated onto glass substrates were done for the determination of the formation of Nickel and cobalt nanoparticles by an X'Pert Pro PANalytical X-ray diffractometer instrument with X'Pert high score plus software operating at a voltage of 45 kV and a current of 40 mA with Cu $K\alpha$ radiation.

2.3 BET Specific Surface Area Analysis

BET (Brauner-Emmett-Teller) specific surface area analysis used physical adsorption of nitrogen gas molecules onto the material surface to calculate surface area. For each material studied, a sample was weighed and placed in a sample cell that was volume calibrated. The sample was heated to the highest acceptable temperature for the particular material and degassed overnight. Nitrogen adsorption isotherms were collected using the seven-point N_2 -BET method to calculate the SSA. For the cobalt and nickel nanoparticles samples, BET analysis was carried out before and after calcinations to remove the template in order to measure both external and total SSA.

2.4 Scanning Electron Microscopy (SEM-EDX)

The morphology and size of particles was characterized using scanning electron microscope (SEM) (JSM-6610 LV) equipped with an energy dispersive X-ray (EDS) spectrophotometer and operated at 20kV.

2.5 Diffuse Reflectance (DRS-UV-visible) Spectroscopy

The Diffuse reflectance spectra (DRS) were recorded with a Shimadzu 3600 UV-Visible NIR spectrophotometer equipped with an integrating sphere diffuse reflectance accessory, using BaSO_4 as reference scatter. Powder samples were loaded into a quartz cell and spectra were recorded in the range of 200-900 nm.

3 Results and Discussion

The experimental powder diffraction (XRD) pattern of the prepared nickel and cobalt nanoparticles is shown in Figure 1. In the XRD (A) pattern of Nickel oxide nanoparticles, diffraction peaks at 37.3112° , 43.2841° , 62.9449° and 75.5188° can be assigned to face-centered cubic (fcc) nickel oxide (111), (200) and (220), (311) and (222) facets of the nickel crystal and 28.278° , 36.0° and 42.112° assigned peaks (111), (311) and (200) facets of the cobalt oxide crystals. Whereas any peaks

originating from potential nickel and cobalt metals cannot be observed. It was observed that the peak intensity increase with a narrowing down particle size distribution with high purity on calcination (Venkatnarayan et al. 2006). In addition to the Bragg peaks representative of fcc nickel and cobalt nanocrystals, additional, and yet unassigned, peaks were also observed suggesting that the crystallization of bio-organic phase occurs on the surface of the silver. The broadening of the Bragg peaks indicates the formation of nanoparticles. The size of the nanoparticles was calculated through the Scherrer's equation (Yuanchun et al. 2008)

$$D = 0.94 \lambda / \beta \cos \theta \quad (1)$$

where D is the average crystallite domain size perpendicular to the reflecting planes, λ is the X-ray wavelength, β is the Full Width at Half Maximum (FWHM), and θ is the diffraction angle. To eliminate additional instrumental broadening the FWHM was corrected, using the FWHM from a large grained Si sample.

$$\beta \text{ corrected} = (\text{FWHM}_{\text{sample}}^2 - \text{FWHM}_{\text{Si}}^2)^{1/2} \quad (2)$$

This modified formula is valid only when the crystallite size is smaller than 100 nm (Patterson 1939).

Figure 2(A) and **(B)** show the typical bright-field SEM micrographs of the synthesized cobalt and nickel oxide nanoparticles. The image 3(A) shows that cobalt oxide nanoparticles are in the form of nanodots. **Figure 2 (B)** shows that nickel oxide nanoparticles are agglomerated and in the form of aggregates. These images suggest that the particles are polydisperse and are mostly spherical in shape. Hence it may be understood that the experimental conditions (viz., pH, temperature and the optimum concentration of NiO and CoO etc.) will achieve the mono-dispersity and uniform shape. A few agglomerated nanoparticles were also observed in some places, thereby indicating possible sedimentation at a later time. It is evident that there is variation in particle sizes and the average size estimated was ~40 nm and ~46 nm for nickel nanoparticles (NiNPs) and cobalt nanoparticles (CoNPs) respectively. It was observed as the temperature increases the crystalline nature of the particle changes with the help of nucleation (Jain et al. 2009). The biological molecules could possibly perform dual functions of formation and stabilization of nickel and cobalt nanoparticles in the aqueous medium. The elemental analysis of cobalt oxide and nickel oxide nanoparticles are reported by EDX and represented by

Figure 3 (A) & (B) The EDX spectrum of cobalt oxide shows the presence of Co and O atoms and the EDX image of nickel Oxide verifies the presence of Ni and O atoms.

The surface area and pore volume was found to be 40.548m²/g and 10.87cm³/g for Cobalt and 50.66 and 8.90 for nickel nanoparticles respectively supporting the presence of limited porosity with a pore size distribution. These values support their industrial applications as a catalyst in organic reactions (Venkatnarayan et al. 2006).

The diffuse reflectance spectra were used to calculate the optical band gap energy of NiO and CoO nanoparticles shown in

Figure 5. The band gap energy was calculated by using Kubelka-Munk Function.

$$F(R) = \frac{(1-R)^2}{2R} \quad (3)$$

Where 'R' is the absolute reflectance of samples and F(R) is the Kuelka-Munk function for the direct band gap of nanoparticles NiO and CoO are direct band gap materials. Where F(R) is plotted against Energy (Eg), the linear extrapolation of the plot to the base line gives the value of band gap energies thus calculated for nanoparticles using the relation(Murphy 2007).

$$E_g = \frac{1240}{\lambda} \quad (4)$$

Figure 4 shows band gaps of NiO and CoO respectively. For NiO direct allowed band gap is 3.47 eV and for CoO the band gap is 1.46 eV. These band gaps energies are higher than the bulk energies for NiO and CoO which indicates that the particles are in nano scale.

Conclusions

Our findings could be targeted for the promising potential applications including industrial organic wastes into biofuel, used lubricating oil into diesel, biosensing devices, and nanoelectronic because of its pollution free and eco-friendly approach. This green synthesis approach shows that the environmentally benign and renewable pomegranate peels and microorganism (fungus) can be used as an effective stabilizing as well as reducing agent for the synthesis of cobalt oxide and nickel oxide nanoparticles respectively. Nickel oxide and cobalt oxide nanoparticles synthesized by this approach are quite stable and no visible changes are observed even after a month. Synthesis of nickel oxide and cobalt oxide nanoparticles using pomegranate peels and fungal biomass are an alternative to chemical synthesis. We anticipate that the smaller particles are mostly stabilized by alkaloids and proteins. Further experiments for the systematic mode of mechanism of size selective synthesis of nickel oxide and cobalt oxide nanoparticles using this very useful pomegranate peels and fungus are in progress.

ACKNOWLEDGEMENTS

The lab facilities of Department of Chemistry, Quaid-I-Azam University, Islamabad and National Center of Physics campus of Quaid-i-Azam University and financial support of the Higher Education of Commission (HEC) of Pakistan is highly acknowledged.

References

- [1]. Murphy, J. C., 2008. Sustainability as an emerging design criterion in nanoparticle synthesis and applications. *J. Mater Chem.* 18, 2173–2176
- [2]. Simone, J. M. D., 2002. Practical Approaches to Green Solvents. *Sc.* 297, 799-803.
- [3]. Singh, R. P., Choi, J. W., 2010. Bio-nanomaterials for versatile bio-molecules detection technology. *Adv. Mater. Letts.* 1, 83-84.
- [4]. Nel, A. E., Mädler, L., Velegol, D., Xia, T., Hoek, E. M. V., Somasundaran, P. I., Klaessig, F., Castranova, V., Thompson, M., 2009. Understanding biophysicochemical interactions at the nano-bio interface. *Nat. Mater.* 8, 543-557.
- [5]. Jamieson, T., Bakhshi, R., Petrova, D., Pocock, R., Imani, M., Seifalian, A. H., 2007. Biological applications of quantum dots. *Biomater.* 28, 4717-4732.
- [6]. Kim, K. Y., 2007. Nanotechnology platforms and physiological challenges for cancer therapeutics. *Nanomed. Nanotech. Biol. Med.* 3, 103-110.
- [7]. Chen, Y., Bangall, D. M., Koh, H. J., Park, K. T., Hiraga, K., Zhu, Z., Yao, T., 1998. Plasma assisted molecular beam epitaxy of ZnO on c-plane sapphire: Growth and characterization. *J. Appl. Phys.* 84, 3912-3918.
- [8]. Wahab, R., Kim, Y. S., Hwang, I. H., Shin, H. S., 2009. A non-aqueous synthesis, characterization of zinc oxide nanoparticles and their interaction with DNA. *Synth. Met.* 159, 2443-2452.
- [9]. Jin, B. J., Bae, S. H., Lee, S. Y., Im, S., 2000. Effects of native defects on optical and electrical properties of ZnO prepared by pulsed laser deposition. *Mater. Sci. Eng. B.* 71, 301-305.
- [10]. Chung, S. W., Yu, J. Y., Health, J. R., 2000. Silicon nanowire devices. *Appl. Phys. Lett.* 76, 2068-2070.
- [11]. Sberveglieri, G., Gropelli, S., Nelli, P., Tintinelli, A., Giunta, G. A., 1995. Novel method for the preparation of NH₃ sensors based on ZnO-In thin films. *Sens. Actuators B.* 25, 588-590.
- [12]. Dahl, A. J., Maddux, S. L. B., Hutchison, E. J., 2007. Toward Greener Nanosynthesis, *Chem. Rev.* 107, 2228-2269.
- [13]. Mao, Y., Park, T.-J., Zhang, F., Zhou, H., Wong, S. S., 2007. Environmentally Friendly Methodologies of Nanostructure Synthesis, *Green nanoChem.* 3, 1122-1139.
- [14]. Colvin, V. L., 2003. The potential environmental impact of engineered nanomaterials, *Nat. Biotechnol.* 21, 1166-1170.
- [15]. Albrecht, A. M., Evans, W. C., Ralston, L. C., 2006. Green chemistry and the health implications of nanoparticles. *Green Chem.* 8, 417-432.
- [16]. Bhainsa, C. K., D'Souza, F. S., 2006. Extracellular biosynthesis of silver nanoparticles using the fungus *Aspergillus fumigatus*. *Colloids and Surfaces B: Biointerfaces*, 47, 160–164.
- [17]. Silva, M. C. C., Silva, A. B. D., Teixeira, F. M., Sousa, P. C. P. D., Rondon, R. M. M., Júnior, J. E. R. H., Sampaio, L. R. L., Oliveira, S. L., Holonda, A. N. M., Vasconcelos, S. M. M. D., 2010. Therapeutic and biological activities of *Calotropis procera* (Ait.) R. Br. *Asian Pacific J. Trop. Med.* 3, 332-336.
- [18]. Venkatnarayan, R., Kanniah, V., Dhathathreya, A., 2006. Tuning size and catalytic activity of nano-clusters of cobalt oxide. *J. Chem. Sci.* 188, 179-184.
- [19]. Yuanchun, Q., Yanbao, Z., Zhishen, W., 2008. Preparation of cobalt oxide nanoparticles and cobalt powders by solvothermal process and their characterization. *Mater. Chem. Phys.* 110, 457-462.
- [20]. Smatt, H. J., Spliethoff, B., Rosenholm, B. J., Linden, M., 2004. Hierarchically porous nanocrystalline cobalt oxide monoliths through nanocasting. *Chem. Comm.* 2188-2189.
- [21]. Devi, R. S. B., Raveendran, R., Vaidyan, V. A., 2007. Synthesis and characterization of Mn²⁺-doped ZnS nanoparticles. *Pramana*, 68, 679-687.
- [22]. Patterson, A., 1939. The Scherrer formula for X-ray particle size determination. *Phys. Rev.* 56, 978–982.
- [23]. Jain, D., Daima, K. H., Kachhwaha, S., Kothari, L. S., 2009. Synthesis of plant-mediated silver nanoparticles using papaya fruit extract and evaluation of their anti microbial activities. *Digest Journal of Nanomaterials and Biostructures.* 4, 557 – 563.
- [24]. Zonooz, F., Salouti, N., 2011. Extracellular biosynthesis of silver nanoparticles using cell filtrate of *Streptomyces* sp. *ERI-3 Scientia Iranica F*, 18, 1631–1635.
- [25]. Venkatnarayan, R., Kanniah, V., Dhathathreya, A., 2006. Tuning size and catalytic activity of nano-clusters of cobalt oxide. *J. Chem. Sci.* 188, 179-184.
- [26]. Murphy, A. B., 2007. Band-gap determination from diffuse reflectance measurements of semiconductor films, and application to photoelectrochemical water-splitting. *Solar Energy Materials and Solar Cells*, 91, 1326-1337.

Figure Captions

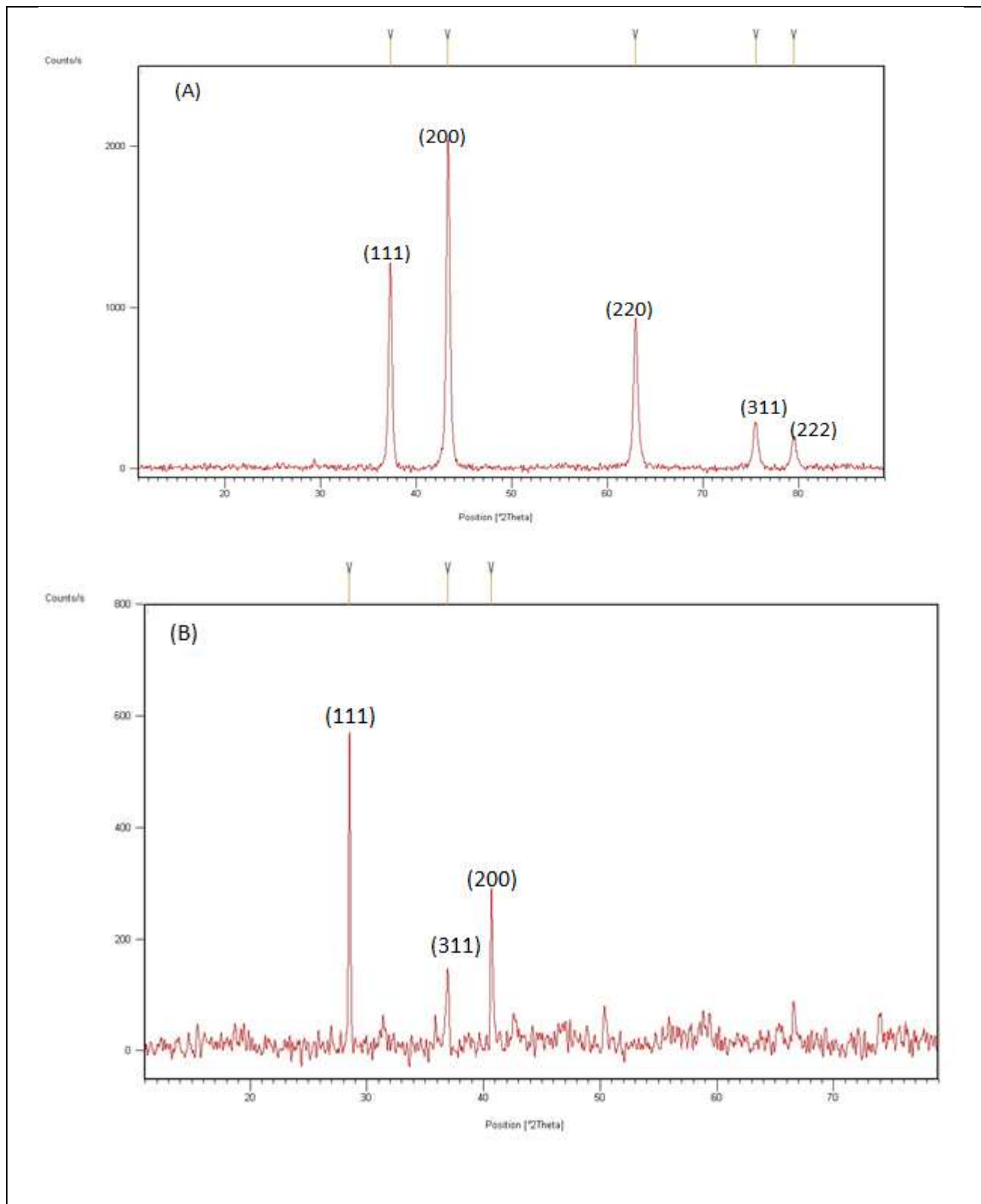


Figure 1 ; XRD of (A) cobalt oxide nanoparticles by pomegranate and (B) nickel oxide nanoparticles by fungal biomass

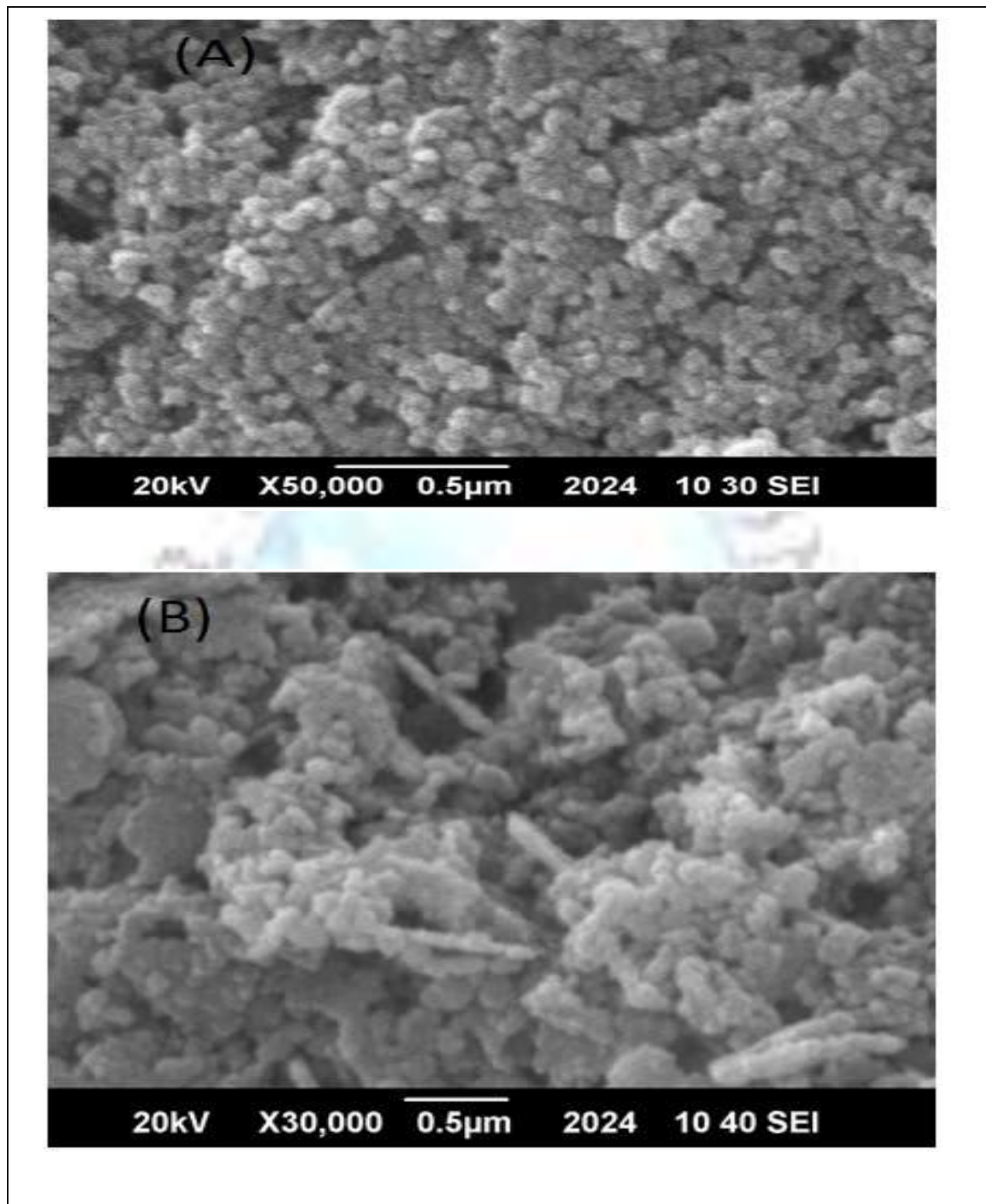


Figure 2 SEM images of (A) nickel oxide nanoparticles produced by pomegranate and (B) cobalt oxide nanoparticles synthesized by fungal biomass

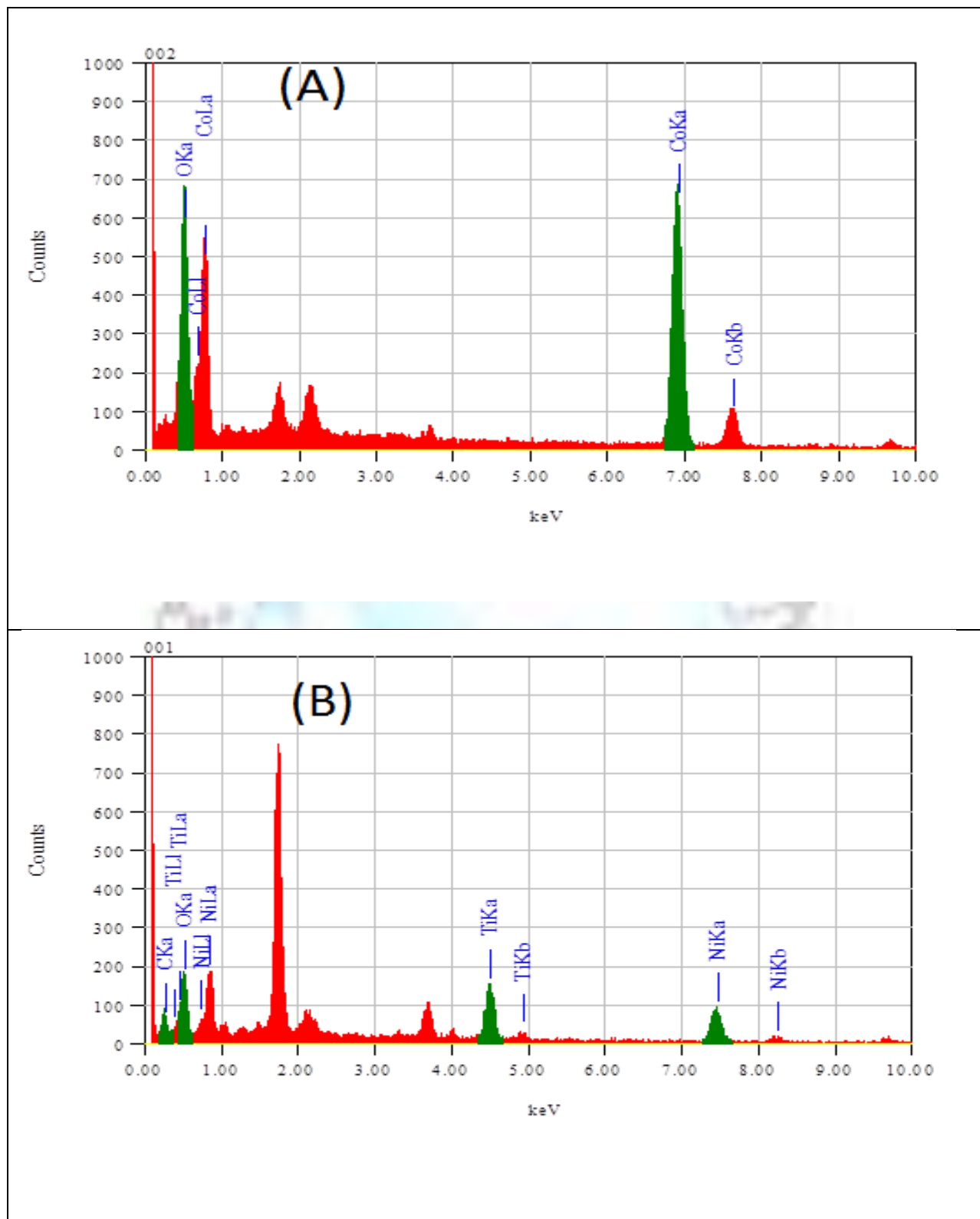


Figure 3 (A) Energy Dispersive X-rays (EDX) spectrograph of cobalt oxide nanoparticles

Figure 3 (B) Energy Dispersive X-rays (EDX) spectrograph of nickel oxide nanoparticles.

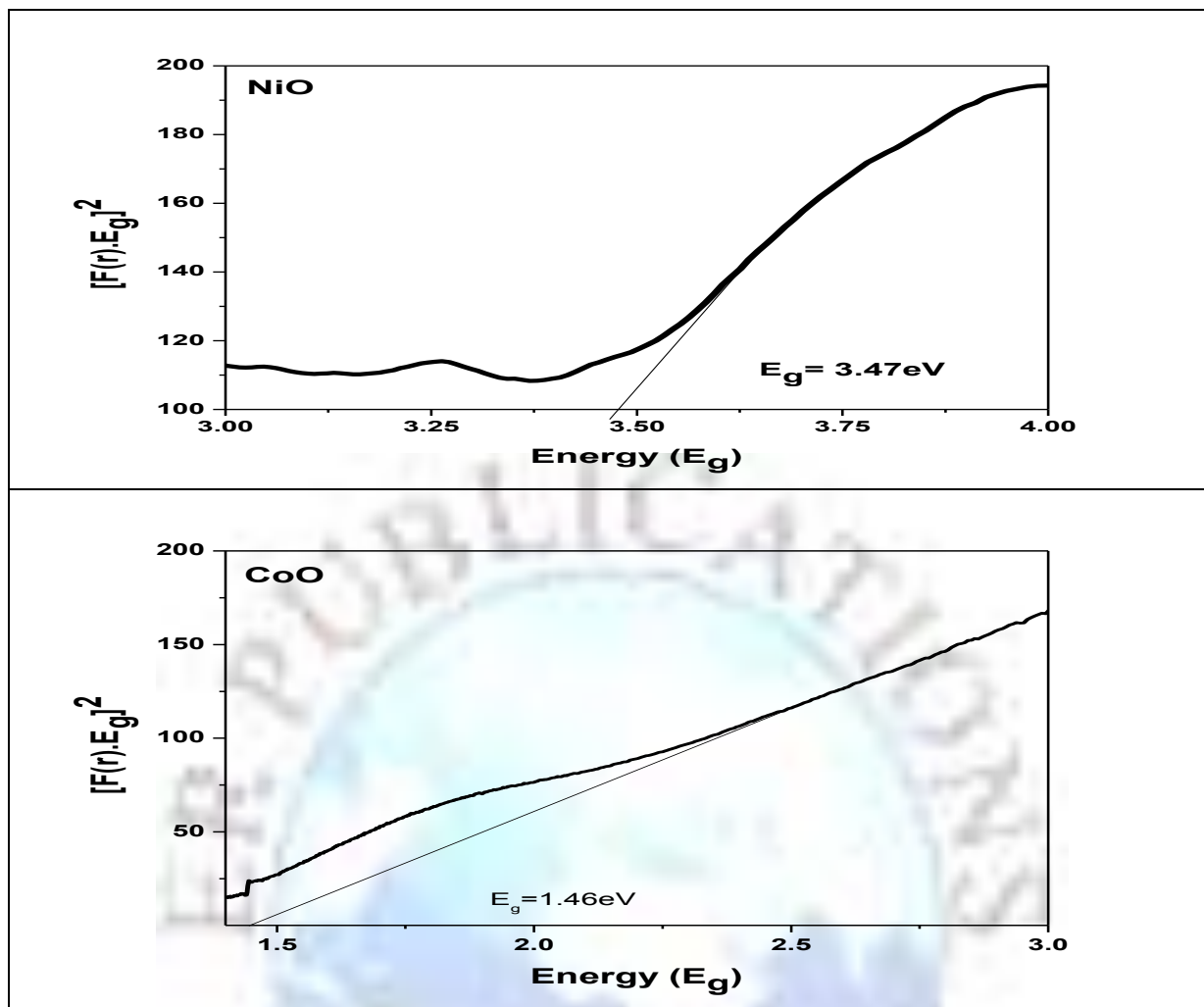


Figure 4: Plot of $[F(r)E_g]^2$ vs Energy (E_g) for NiO and CoO nanoparticles

Table. 1. This table shows various properties of nickel and cobalt nanoparticles

Method	Metal oxide NPs	BET S.A m^2g^{-1}	Langmuir S.A m^2g^{-1}	Pore Volume cm^3g^{-1}	Pore size cm^3g^{-1}	Average Particle size nm
Pomegranate biomass	Nickel	40.548	32.678	10.87	18.72	40
Fungal Biomass	Cobalt	50.66	48.583	8.90	18.72	46